Stress Intensity Factor Error Index for Finite Element Analysis with Singular Elements

T. Meshii, et al., Engineering Fracture Mechanics, Vol. 70, No. 5, pp. 657-669 (2002. 3).

Stress Intensity Factor Error Index for Finite Element Analysis with Singular Elements

Toshiyuki MESHII[a]*and Katsuhiko WATANABE[b]

[a*] Department of Mechanical Engineering, Fukui University, 3-9-1, Bunkyo, Fukui, Fukui, 910-8507, Japan
Phone: +81-776-27-8468, Fax: +81-776-27-8468, E-mail : meshii@mech.fukui-u.ac.jp

[b] 1st Division, Institute of Industrial Science, University of Tokyo, 4-6-1, Komaba, Meguro-ku, Tokyo, 153-8505, Japan

Abstract

An error index for the stress intensity factor (SIF) obtained from the finite element analysis (FEA) results using singular elements is proposed. The index was developed by considering the facts that the analytical function shape of the crack tip displacement is known and that the SIF can be evaluated from the displacements only. The advantage of the error index is that it has the dimension of the SIF and converges to zero when the actual error of the SIF by displacement correlation technique converges to zero. Numerical examples for some typical crack problems, including a mixed mode crack, whose analytical solutions are known, indicated the validity of the index. The degree of actual SIF error seems to be approximated by the value of the proposed index.

Key Words: Fracture Mechanics, Stress Intensity Factor, Finite Element Method, Error Index, Singular Element

1. Introduction

It is popular to evaluate the integrity of a cracked structure under arbitrary loads by comparing the stress intensity factor (SIF) for the crack with the critical value peculiar to the material. The SIF is often evaluated from finite element analysis (FEA) results and is effective particularly when the SIF solution for the crack under specific load condition is not known, while the error estimation of the obtained SIF is very important.

In the past, many techniques have been proposed for FEA of a cracked structure in order to express and evaluate the stress singularity of the stress at the crack tip. Among these, one of the most popular techniques is to apply singular elements, which Barsoum [1] and Henshell and Shaw [2] proposed independently, to realize the crack tip stress singularity. In this case, the SIF is usually evaluated by Tracey's formula [3] (Displacement Correlation Technique, hereafter referred to as DCT). The feature of this

technique is that a SIF of practical accuracy can be obtained by comparatively coarse mesh division. So, many researchers have been trying to answer the question "how coarse the singular element can be to secure the SIF accuracy?" However, it has become known that the load conditions as well as the singular element size affect the SIF accuracy. Thus, it is generally accepted that an optimum singular element size that satisfies arbitrary conditions does not exist [4].

Generally the accuracy of the SIF solution by FEA is improved by increasing the number of elements. However, since it is an engineering problem (and especially to take advantages of singular elements), it is desirable to obtain sufficiently accurate SIF by a mesh division as coarse as possible. This will be possible if we can estimate the error of the SIF obtained from one trial analysis. We can make corrections or judge whether the obtained SIF solution is applicable from a practical viewpoint. Fuenmayor et al. [5] applied the error index (expressed through the energy norm) which Zienkiewicz and Zhu [6] proposed for estimating errors in FEA results. However, since the error index is not expressed in terms of the SIF, one can only expect that the SIF error will be small when the index becomes small. We cannot know the degree of the actual SIF error. So we developed a new SIF error index that has the dimension of the SIF, based on the following three facts: (i) The analytical function form of the crack tip displacements is known. (ii) Though incomplete, displacements on a singular element represent a part of the analytical displacement distribution. (iii) The SIF can be evaluated from the displacements of crack tip elements.

In the following, we will first explain the concept of the error index which we have developed, and then demonstrate its validity by comparing our error index with the actual error for three typical crack problems whose analytical solutions are known.

2. Proposal of DCE (Displacement Correlation Error) index

Consider a polar-coordinate system (r, θ) as shown in Fig. 1 where the crack tip is chosen as the origin and the crack surfaces as $\theta=\pm\pi$. The asymptotic solutions of displacement around the crack tip are generally given by

$$\begin{Bmatrix} u \\ v \end{Bmatrix} = \begin{Bmatrix} u_0 \\ v_0 \end{Bmatrix} + \frac{r^{n/2}}{2G} \sum_{n=1}^{\infty} \left(A_{\mathrm{I}n} \begin{Bmatrix} f_{\mathrm{I}un}(\theta) \\ f_{\mathrm{I}vn}(\theta) \end{Bmatrix} - A_{\mathrm{II}n} \begin{Bmatrix} f_{\mathrm{II}un}(\theta) \\ f_{\mathrm{II}vn}(\theta) \end{Bmatrix} \right) \quad \cdots\cdots(1)$$

where u_0 and v_0 are the rigid body displacements in x and y directions, respectively, u and v are the displacements in x and y directions, respectively, G is the shearing modulus and

$$\begin{Bmatrix} f_{\mathrm{I}u n}(\theta) \\ f_{\mathrm{I}v n}(\theta) \\ f_{\mathrm{II}u n}(\theta) \\ f_{\mathrm{II}v n}(\theta) \end{Bmatrix} = \begin{Bmatrix} -\frac{n}{2}\cos\left(\frac{n}{2}-2\right)\theta + \left(\kappa+\frac{n}{2}+(-1)^n\right)\cos\frac{n\theta}{2} \\ \frac{n}{2}\sin\left(\frac{n}{2}-2\right)\theta - \left(-\kappa+\frac{n}{2}+(-1)^n\right)\sin\frac{n\theta}{2} \\ -\frac{n}{2}\sin\left(\frac{n}{2}-2\right)\theta + \left(\kappa+\frac{n}{2}-(-1)^n\right)\sin\frac{n\theta}{2} \\ -\frac{n}{2}\cos\left(\frac{n}{2}-2\right)\theta - \left(\kappa-\frac{n}{2}+(-1)^n\right)\cos\frac{n\theta}{2} \end{Bmatrix} \quad \text{.....(2)}$$

Here, suffixes I and II indicate the quantities corresponding to mode I and mode II deformations, respectively, and suffixes u and v represent the quantities corresponding to the displacements u and v, respectively. Letting ν be the Poisson's ratio, κ is $(3-4\nu)$ for plane strain or $(3-\nu)/(1+\nu)$ for plane stress. Accordingly, when we think of the relative displacements $u^*(r, \theta)$ and $v^*(r, \theta)$ in x and y directions, respectively, between two symmetric points across the x axis, they can be obtained as [7] , and

$$\begin{Bmatrix} u^*(r,\theta) \\ v^*(r,\theta) \end{Bmatrix} \equiv \begin{Bmatrix} u(r,\theta)-u(r,-\theta) \\ v(r,\theta)-v(r,-\theta) \end{Bmatrix} = \sum_{n=1}^{\infty} \frac{r^{\frac{n}{2}}}{G} \begin{Bmatrix} -A_{\mathrm{II}n} f_{\mathrm{II}u n}(\theta) \\ A_{\mathrm{I}n} f_{\mathrm{I}v n}(\theta) \end{Bmatrix} \quad \text{.....(3)}$$

Note that, since $f_{\mathrm{I}v n}$ and $f_{\mathrm{II}u n}$ are odd functions and $f_{\mathrm{I}u n}$ and $f_{\mathrm{II}v n}$ are even functions, $u^*(r, \theta)$ and $v^*(r, \theta)$ are related to only mode II and mode I deformations, respectively, and the SIFs are defined as $K_{\mathrm{I}} = \sqrt{2\pi}\ A_{\mathrm{I}1}$ and $K_{\mathrm{II}} = -\sqrt{2\pi}\ A_{\mathrm{II}1}$.

On the other hand, when we employ the singular elements in FEA, the displacements $U(r, \theta)$ and $V(r, \theta)$ in x and y directions on the edges in r direction of a singular element can be expressed, by using the nodal displacements of the quarter and the end points, as

$$\begin{Bmatrix} U(r,\theta) \\ V(r,\theta) \end{Bmatrix} = \begin{Bmatrix} U_0 \\ V_0 \end{Bmatrix} + \begin{Bmatrix} -3U_0 + 4U(L/4,\theta) - U(L,\theta) \\ -3V_0 + 4V(L/4,\theta) - V(L,\theta) \end{Bmatrix} \sqrt{\frac{r}{L}} + \begin{Bmatrix} 2U_0 - 4U(L/4,\theta) + 2U(L,\theta) \\ 2V_0 - 4V(L/4,\theta) + 2V(L,\theta) \end{Bmatrix} \frac{r}{L} \quad \text{.....(4)}$$

Here, U_0 and V_0 are the rigid body displacements in x and y directions, respectively. The relative displacements $U^*(r, \theta) \equiv U(r, \theta) - U(r, -\theta)$ and $V^*(r, \theta) \equiv V(r, \theta) - V(r, -\theta)$ can be obtained as

$$\begin{Bmatrix} U^*(\boldsymbol{r},\theta) \\ V^*(\boldsymbol{r},\theta) \end{Bmatrix} = \begin{Bmatrix} 4\boldsymbol{U}^*(\boldsymbol{L}/4,\theta) - \boldsymbol{U}^*(\boldsymbol{L},\theta) \\ 4\boldsymbol{V}^*(\boldsymbol{L}/4,\theta) - \boldsymbol{V}^*(\boldsymbol{L},\theta) \end{Bmatrix} \sqrt{\frac{\boldsymbol{r}}{\boldsymbol{L}}} + \begin{Bmatrix} -4\boldsymbol{U}^*(\boldsymbol{L}/4,\theta) + 2\boldsymbol{U}^*(\boldsymbol{L},\theta) \\ -4\boldsymbol{V}^*(\boldsymbol{L}/4,\theta) + 2\boldsymbol{V}^*(\boldsymbol{L},\theta) \end{Bmatrix} \frac{\boldsymbol{r}}{\boldsymbol{L}} \quad \text{.....(5)}$$

and they also must be related to only mode II and mode I deformations, respectively.

The Tracey's formula [3] is frequently used to evaluate the SIF from FEA results. That is, the SIF K_{DCT} is evaluated by letting Eqn. (5) correspond to the first two terms of Eqn. (3) on the crack surfaces ($\theta = \pi$) and it is given concretely, considering. $f_{\mathrm{I}v1}(\pi) = f_{\mathrm{II}u1}(\pi) = \kappa + 1$, $A_{\mathrm{I}1} = K_{\mathrm{I\,DCT}}/(2\pi)^{1/2}$, $A_{\mathrm{II}1} = -K_{\mathrm{II\,DCT}}/(2\pi)^{1/2}$ and setting $G' \equiv (2\pi/L)^{1/2} G/(1+\kappa)$, as

$$\begin{Bmatrix} K_{\mathrm{II\,DCT}} \\ K_{\mathrm{I\,DCT}} \end{Bmatrix} = G' \begin{Bmatrix} 4U^*(L/4,\pi) - U^*(L,\pi) \\ 4V^*(L/4,\pi) - V^*(L,\pi) \end{Bmatrix} \quad \cdots\cdots(6)$$

Note that the K_{DCT} in Eqn. (6) is evaluated for $\theta=\pi$. It generally differs from the SIF evaluated in a similar way for other $\theta(\neq\pi)$, because singular element displacements are not guaranteed to satisfy the angular characteristics of asymptotic solutions. When we think of a sufficiently small region around a crack tip, terms higher than $O(r^{3/2})$ can be neglected in Eqn. (3). The relative displacements can be accurately expressed by the first two terms of Eqn. (3). If the true SIFs K_{I} and K_{II} are known, Eqn. (3) can be deduced for the crack surfaces, with $f_{\mathrm{I}\,v2}(\pi)=0$ and $f_{\mathrm{II}\,u2}(\pi)=0$, as follows.

$$\begin{Bmatrix} u^*(r,\pi) \\ v^*(r,\pi) \end{Bmatrix} = \frac{1}{G'}\sqrt{\frac{2\pi r}{L}} \begin{Bmatrix} -A_{\mathrm{II}\,1} \\ A_{\mathrm{I}1} \end{Bmatrix} = \frac{1}{G'}\sqrt{\frac{r}{L}} \begin{Bmatrix} K_{\mathrm{II}} \\ K_{\mathrm{I}} \end{Bmatrix} \quad \cdots\cdots(7)$$

On the other hand, the corresponding expressions $U^*(r, \pi)$ and $V^*(r, \pi)$ for the singular elements are deduced by substituting the SIFs $K_{\mathrm{I\,DCT}}$ and $K_{\mathrm{II\,DCT}}$ into Eqn. (6), as

$$\begin{Bmatrix} U^*(r,\pi) \\ V^*(r,\pi) \end{Bmatrix} = \frac{1}{G'}\sqrt{\frac{r}{L}} \begin{Bmatrix} K_{\mathrm{II\,DCT}} \\ K_{\mathrm{I\,DCT}} \end{Bmatrix} + \frac{2r}{L} \begin{Bmatrix} U^*(L,\pi) - 2U^*(\frac{L}{4},\pi) \\ V^*(L,\pi) - 2V^*(\frac{L}{4},\pi) \end{Bmatrix} \quad \cdots\cdots(8)$$

The nodal displacements in FEA are obtained by determining the unknown coefficients in the adopted displacement function through potential energy minimization process and Eqn. (5) does not necessarily coincide with Eqn. (3). Thus, the coefficients of r/L in Eqn. (8) are not zero unless the adopted displacement function can express the true displacement solution. However, since the singular elements under consideration are conformal elements [1], FEA displacements tend to the exact solutions when the size of the elements approaches zero (note that the element size has to be decreased not only in the r direction but also in the θ direction). Then, the second term in Eqn. (8) converges to zero and K_{DCT} to the true value. This suggests the possibility of the second term in Eqn. (8) to become a SIF error index. We will now multiply the coefficient for r/L in Eqn. (8) with $(-G'/2)$ and name the quantity defined by

$$\begin{Bmatrix} \Delta K_{\mathrm{I\,DCE}} \\ \Delta K_{\mathrm{II\,DCE}} \end{Bmatrix} = G' \begin{Bmatrix} 2V^*(L/4,\pi) - V^*(L,\pi) \\ 2U^*(L/4,\pi) - U^*(L,\pi) \end{Bmatrix} \quad \cdots\cdots(9)$$

DCE index (Displacement Correlation Error Index) ΔK_{DCE}.

Strong points of the DCE index, the proposed error index, are that (1) it can be directly calculated from the nodal displacements on the singular elements, (2) it converges to zero when the size of the singular elements approaches zero and (3) it has the dimension of a SIF. Thus, the DCE index differs from conventional error indexes, which generally focus on the convergence during iterative mesh refinements. The DCE index may give a SIF error estimate from a single FEA result. This suggests the possibility of dramatically reducing efforts and costs in SIF analysis.

3. Numerical examples

In this section, FEA for three typical crack problems, whose analytical SIF solutions K_{ref} are known, were conducted by using singular elements. The error defined as the difference between K_{DCT} computed with DCT (Eq. (6)) and K_{ref}, $K_{error}=(K_{DCT}-K_{ref})$, was compared with the corresponding ΔK_{DCE}. In all cases, shearing modulus G of 79 GPa and Poisson's ratio ν of 0.3 were used. In order to investigate the effect of singular element size, analyses were carried out changing the number m and the length L (see Fig.1) of singular elements. m was 8 [8], 16, 24 and 30, and L/a was taken at 1/3, 1/6, 1/12 and 1/24 for each m, letting it roughly correspond to the guideline proposed in the early days (L/a=0.05～0.2) [8] .

3.1 Single edge cracked beam under uniform tension

The single edge cracked beam under uniform stress σ= 9.8 MPa in the left of Fig. 2 was considered first. The dimensions of the beam were W=10 mm wide, $H = 2W$ = 20 mm high and crack length was a = 1 or 3 mm. K_{Ierror} was obtained by using the following $K_{I\,ref}$ [9] and was compared with $\Delta K_{I\,DCE}$.

$$K_{I\,ref}(\xi=\frac{a}{W})=\sigma\sqrt{\pi a}\times\sqrt{\frac{2}{\pi\xi}\tan\frac{\pi\xi}{2}}\cdot\frac{0.752+2.02\xi+0.37\{1-\sin(\pi\xi/2)\}^3}{\cos(\pi\xi/2)} \quad \text{..... (10)}$$

As is discussed in the next paragraph, the dependence of the results on the value of m in this problem can be regarded sufficiently small when we choose m to be 16 or more. Thus, the results for the case of m = 16 are shown in Fig. 2 and Tab. 1. The differences between K_{Ierror} and $\Delta K_{I\,DCE}$ can be read directly from the figure as the vertical distance between a mark and a line of unit slope crossing the origin. For example, the maximum difference between K_{Ierror} and $\Delta K_{I\,DCE}$ in this figure is found to be 0.0156 (1.56% of $K_{I\,ref}$) for the mark corresponding to the result when a/W = 0.1 and L/a = 1/3. This figure shows that $\Delta K_{I\,DCE}$

decreases when L/a becomes small and, at the same time, $K_{\mathrm{I\,error}}$ decreases. The difference between $\Delta K_{\mathrm{I\,DCE}}$ and $K_{\mathrm{I\,error}}$ seems to be small in the range shown in the figure.

The dependence of the relation between ΔK_{DCE} and K_{error} on m is shown in Figs. 3 and 4 for mode I and mode II components, respectively, for the case of $a/W = 0.1$. The concrete values of data in Figs. 3 and 4 are summarized in Tabs. 2 and 3, respectively. Here, the analytical SIF for mode II for this problem is zero, so that $K_{\mathrm{II\,error}} = K_{\mathrm{II\,DCT}}$. Therefore, $\sigma(\pi a)^{1/2}$ was used to normalize $K_{\mathrm{II\,error}}$ and $\Delta K_{\mathrm{II\,DCE}}$ in Fig. 4. We see from Fig. 4 that the increase of m does not necessarily lead to the decrease of $K_{\mathrm{II\,error}}$. This seems due to the fact that the mode II SIF is zero. It is considered that, when we take also the results in section 3.3 into consideration, the tendency expected for conformal elements does not appear for small K_{II}, unless both m and L are decreased together smoothly and appropriately. On the other hand, we see from Fig. 3 that, if we choose m to be 16 or more, the vertical distance between a mark and a straight line of unit slope crossing the origin (the difference between $K_{\mathrm{I\,error}}$ and $\Delta K_{\mathrm{I\,DCE}}$) becomes approximately constant. Thus, the effect of m on the mode I SIF can be disregarded.

3. 2 Circumferential crack in a cylinder under uniform tension

A circumferential crack in a cylinder under remote uniform stress $\sigma = 9.8$ MPa as in the left of Fig. 5 was considered next. The dimensions of the cylinder were $R_{\mathrm{m}} = 95$ mm in mean radius, W=10 mm thick and $H = 16W = 160$ mm long. The crack length was $a = 1$ or 3 mm. The solution by Nied was adopted as $K_{\mathrm{I\,ref}}$ to evaluate $K_{\mathrm{I\,error}}$ (a/W, $K_{\mathrm{I\,ref}}$ MPam$^{1/2}$) = (0.1, 0.636), (0.3, 1.324) [10] and $K_{\mathrm{I\,error}}$ was compared with $\Delta K_{\mathrm{I\,DCE}}$. The results for the case of $m = 16$ are shown in the right of Fig. 5 and Tab. 4 from the same reason as for the right of Fig. 2. The maximum difference between $K_{\mathrm{I\,error}}$ and $\Delta K_{\mathrm{I\,DCE}}$ in the figure is seen to be 0.67% of $K_{\mathrm{I\,ref}}$ for the mark corresponding to the case where $a/W = 0.1$ and $L/a = 1/3$. Also in this case, $\Delta K_{\mathrm{I\,DCE}}$ decreases when L/a becomes small and, at the same time, $K_{\mathrm{I\,error}}$ decreases. The difference between $\Delta K_{\mathrm{I\,DCE}}$ and $K_{\mathrm{I\,error}}$ seems to be small in the range shown in the figure.

The dependence of the relation between ΔK_{DCE} and K_{error} on m is shown in Figs. 6 and 7 for mode I and mode II components, respectively, for the case of $a/W = 0.1$. The concrete values for data in Figs. 6 and 7 are given in Tabs. 5 and 6, respectively. Here, the analytical SIF for mode II is zero, so that $K_{\mathrm{II\,error}} = K_{\mathrm{II\,DCT}}$. Therefore $\sigma(\pi a)^{1/2}$ was used again to

normalize $K_{\mathrm{II\ error}}$ and $\Delta K_{\mathrm{II\ DCE}}$ in Fig. 7. We see from Fig. 7 that the increase of m does not necessarily contribute to the decrease of $K_{\mathrm{II\ error}}$ similarly as did not in Fig. 4. This seems due to the fact that the mode II SIF is zero also for this problem. It seems that the tendency expected for conformal elements does not appear for small K_{II}, unless both m and L are decreased together smoothly and appropriately. On the other hand, we see from Fig. 6 that, if we choose m to be 16 or more, the vertical distance between a mark and a line of unit slope crossing the origin (the difference between $K_{\mathrm{I\ error}}$ and $\Delta K_{\mathrm{I\ DCE}}$,) becomes approximately constant. Thus, the effect of m on the mode I SIF can be disregarded.

3. 3 Center slant cracked rectangular plate subjected to uniform tension

The problem of a center slant cracked rectangular plate under uniform stress σ= 9.8 MPa in Fig. 8 left was considered. The dimensions of the plate were $2W$ = 30 mm wide and $2H$ = 60 mm high. Crack length was $2a$ = 6 or 12 mm and crack inclination angle was α=30°. K_{error} was obtained by comparing with Kitagawa's analytical solution (($K_{\mathrm{I\ ref}}$, $K_{\mathrm{II\ ref}}$) = (0.735, 0.415) and (1.138, 0.605) MPam$^{1/2}$ for a/W = 0.2 and 0.4, respectively)[11] and was compared with ΔK_{DCE} in the right of Fig. 8 and Tab. 7. The results for m = 24 are shown in Fig.8 and the effects of m on K_{DCT} for the case of a/W = 0.4 are summarized in Fig. 9 and Tab. 8. As we see from Fig.9, there is a difference of up to 2.74% between the mode I $\Delta K_{\mathrm{DCE}}/K_{\mathrm{ref}}$ and mode II $\Delta K_{\mathrm{DCE}}/K_{\mathrm{ref}}$ for m = 8. This is thought of unfavorable because we estimate each SIF and error from one FEA. Thus, we set a guideline for this mode I and II $\Delta K_{\mathrm{DCE}}/K_{\mathrm{ref}}$ difference to be lower than 1.5% and the results for m = 24 are shown in Fig. 8. Note that the mode I $\Delta K_{\mathrm{DCE}}/K_{\mathrm{ref}}$ changes slightly as m increases. The maximum difference between K_{error} and ΔK_{DCE} in Fig. 8 can be read as 3.40% of K_{ref} for mode II. Both ΔK_{DCE} and K_{error} shows the tendency to decrease while L/a is made small.

4. Discussion

The DCE Index ΔK_{DCE}, which we proposed in this paper, is intended to give an estimate of the error of the SIF evaluated from FEA results by DCT. When we refine the crack tip singular elements in both r and θ directions with proper correlation (that is, when we decrease both L/a and $1/m$ appropriately), the plot (ΔK_{DCE}, K_{error}) is expected to approach the origin in a figure as were shown in previous section. That is, K_{error} is expected to approach zero when ΔK_{DCE} approaches zero. This characteristic of

ΔK_{DCE} is similar to that of the error index proposed in the past [5], [6] which was based on the energy norm. However, we think that ΔK_{DCE} is advantageous because it has the dimension of a SIF and the SIF error can be discussed directly.

In order to make full use of the merit of ΔK_{DCE} mentioned above, we had better reduce the element size in both r and θ directions properly by correlating two parameters L/a and $1/m$. However, because this makes the finite element division quite difficult, we first fixed the number of elements in θ direction m and reduced the element size in r direction in the numerical examples shown in the previous section. The results showed that K_I is relatively insensitive to mesh refinements in θ direction, thus, in the evaluation of K_I, we can concentrate on refining the mesh in r direction once we choose m larger than a certain value. On the other hand, the situation differs with regard to K_{II}; that is, the convergence of K_{II} by varying m should be confirmed. In any case, the validity of m can be judged by how the plots on a figure like Fig. 9 point to the origin with the decrease of L/a in the analysis of a problem of which the analytical SIF solutions are known. The value of m used in the numerical examples in this paper seems to be valid at least in K_I evaluation that is important in many cases. Note that our error index takes the value of the same degree as that of the SIF error itself in the region of $|\Delta K_{I\,DCE}/K_{I\,ref}| < 0.05$. It is in the evaluation of SIF, essentially, for the problem whose analytic solution is not known that the error index can play its role. The results here for K_I shows, while some more study might be necessary, that, when we choose $m \geq 16$ and consider the range of $|\Delta K_{I\,DCE}/K_{I\,DCT}| < 0.05$ instead of $|\Delta K_{I\,DCE}/K_{I\,ref}| < 0.05$, there is a possibility to estimate the degree of the error itself by our error index and, by using it, compensate the error in $K_{I\,DCT}$. Regarding to K_{II}, as shown in Fig. 9, the plot of $(K_{error}, \Delta K_{DCE})$ moves closer to the origin with the increase of m when L/a is made small. From this, we may be able to expect that an error estimation procedure similar to that for K_I just mentioned can be applied to also K_{II}, if we use large m. However, the employment of large m is not necessarily realistic and it may be said in this sense that the singular element is not necessarily suitable for K_{II} evaluation. Even if so, the discrepancy in accuracy of K_I and K_{II} is not desirable generally in the analysis of a mixed mode crack problem and the magnitude of $|\Delta K_{I\,DCE}/K_{I\,ref} - \Delta K_{II\,DCE}/K_{II\,ref}|$ can be used as a measure to judge the validity of employed m as was shown in section 3.3. When the analytical solution is not known, $|\Delta K_{I\,DCE}/K_{I\,DCT} - \Delta K_{II\,DCE}/K_{II\,DCT}|$ can be used instead.

Recently, Rahulkumar et al. [12] proposed an approach to use higher order singular elements for an accurate SIF evaluation with a coarse mesh division. However, judging from the results of a mixed mode problem discussed in section 3.3, it still remains necessary to try to find a proper mesh refinement in θ direction (selection of m) even though higher order elements are used. Also for this case, it will be effective to select m first for Barsoum's singular element by applying ΔK_{DCE} as proposed in this paper.

5. Conclusions

An error index for SIF obtained from the FEA results using singular elements was developed and was named DCE (Displacement Correlation Error) index. The DCE index was developed as a SIF error index that has the dimension of a SIF, based on the following three facts: (i) The analytical functional form of the crack tip displacements is known. (ii) Though incomplete, displacements on a singular element represent a part of the analytical displacement distribution. (iii) The SIF can be evaluated from the displacements of crack tip elements. Although the DCE index is not the SIF error itself, the presented numerical results (for the problems whose analytical solutions are known) for appropriate mesh divisions in θ direction showed that the DCE index is close to the actual SIF error, especially for mode I SIF evaluation that is important in most practical problems, and that error compensation by using it might be possible in an engineering sense.

References

[1] Barsoum RS. On the use of isoparametric finite elements in fracture mechanics. Int J Num Meth Engng 1976;10:25-37.

[2] Henshell RD, Shaw KG. Crack tip finite elements are unnecessary. Int J Num Meth Engng 1975;9:495-507.

[3] Tracey DM. Discussion of 'On the use of isoparametric finite elements in fracture mechanics' by RS Barsoum. Int J Num Meth Engng 1976;10:401-403.

[4] Harrop LP. The optimum size of quarter-point crack tip elements. Int J Num Meth Engng 1982;17:1101-1103.

[5] Fuenmayor J, Domínguez E, Giner E, Oliver JL. Calculation of stress intensity factor and estimation of its error by a shape sensivity analysis. Fatigue Fract Engng Mater Struct 1997;20:813-828.

[6] Zienkiewicz OC, Zhu JZ. A simple error estimator and adaptive procedure for practical engineering analysis. Int J Num Meth Engng 1987;24:337-357.

[7] Ishikawa H, Kitagawa H, Okamura H. J integral of a mixed mode crack and its application, In: Proc 3rd Int Conf Mechanical Behaviour of Materials, vol. 3. Oxford, Pergamon Press; 1980. p. 447-455.

[8] Saouma VE, Schwemmer. Numerical evaluation of the quarter point crack tip element. Int J Num Meth Engng 1984;20:1629-1641.

[9] Tada H, Paris PC, Irwin GR. The stress analysis of cracks handbook. 2nd ed. Hellertown: Del Research Corp.; 1985.

[10] Nied, HF, Erdogan F. The elasticity problem for a thick-walled cylinder containing a circumferential crack. Int J Fract 1983;22:277-301.

[11] Murakami, Y. Stress intensity factors handbook. Oxford: Pergamon Press; 1986.

[12] Rahulkumar P, Saigal S, Yunus S. Singular p-version finite elements for stress intensity factor computations. Int J Num Meth Engng 1997;40:1091-1114.

Acnowledgement

We thank the Cornell Fracture Group for their FEA code FRANC2D and their discussion on the subject. We especially thank Dr. C.-S. Chen's effort to add to the code a function to select a number of the singular elements.

NOMENCLATURE

a: crack length

$f_{\mathrm{I}u\,n}, f_{\mathrm{I}v\,n}, f_{\mathrm{II}u\,n}, f_{\mathrm{II}v\,n}$: angular functions corresponding to modes I and II, displacements u and v, and $r^{n/2}$

m: number of singular elements

r, θ: polar coordinates

u, v: displacements in the x and y directions (u_0, v_0: rigid body displacements in the x and y directions; u^*, v^*: relative displacements of two symmetric points across the x axis in the x and y directions)

x, y: Cartesian coordinates

$A_{\mathrm{I}n}, A_{\mathrm{II}n}$: coefficients corresponding to modes I and II, and $r^{n/2}$ in crack tip displacements asymptotic expansion

G: shearing modulus

G': $\equiv (2\pi/L)^{1/2} G/(1+\kappa)$

H: plate height or cylinder length; see Fig. 2, 5 or 8 for details

K_{I}, K_{II}: mode I and II stress intensity factors

K_{IDCT}, K_{IIDCT}: mode I and II stress intensity factors evaluated from FEA results using singular elements

K_{Iref}, K_{IIref}: mode I and II analytical stress intensity factor solutions

K_{Ierror}, K_{IIerror}: mode I and II stress intensity factor errors defined as $K_{\mathrm{error}} = K_{\mathrm{DCT}} - K_{\mathrm{ref}}$

ΔK_{IDCE}, $\Delta K_{\mathrm{IIDCE}}$: mode I and II DCE indexes

L: singular element size

U, V: displacements of singular elements in the x and y directions (U_0, V_0: rigid body displacements in the x and y directions; U^*, V^*: relative displacements of two symmetric points across the x axis in the x and y directions)

W: plate width or cylinder thickness; see Fig. 2, 5 or 8 for details

R_{m}: mean radius

α: crack inclination angle

κ: $(3-4\nu)$ for plane strain or $(3-\nu)/(1+\nu)$ for plane stress

ν: Poisson's ratio

σ: applied stress

List of Figures and Tables

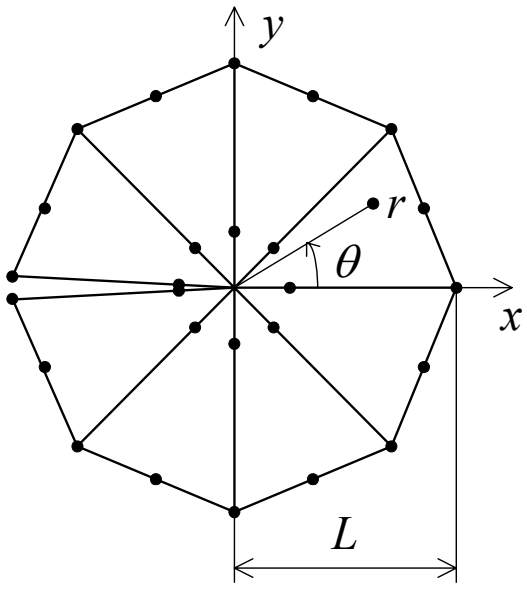

Fig. 1. Singular crack tip elements.

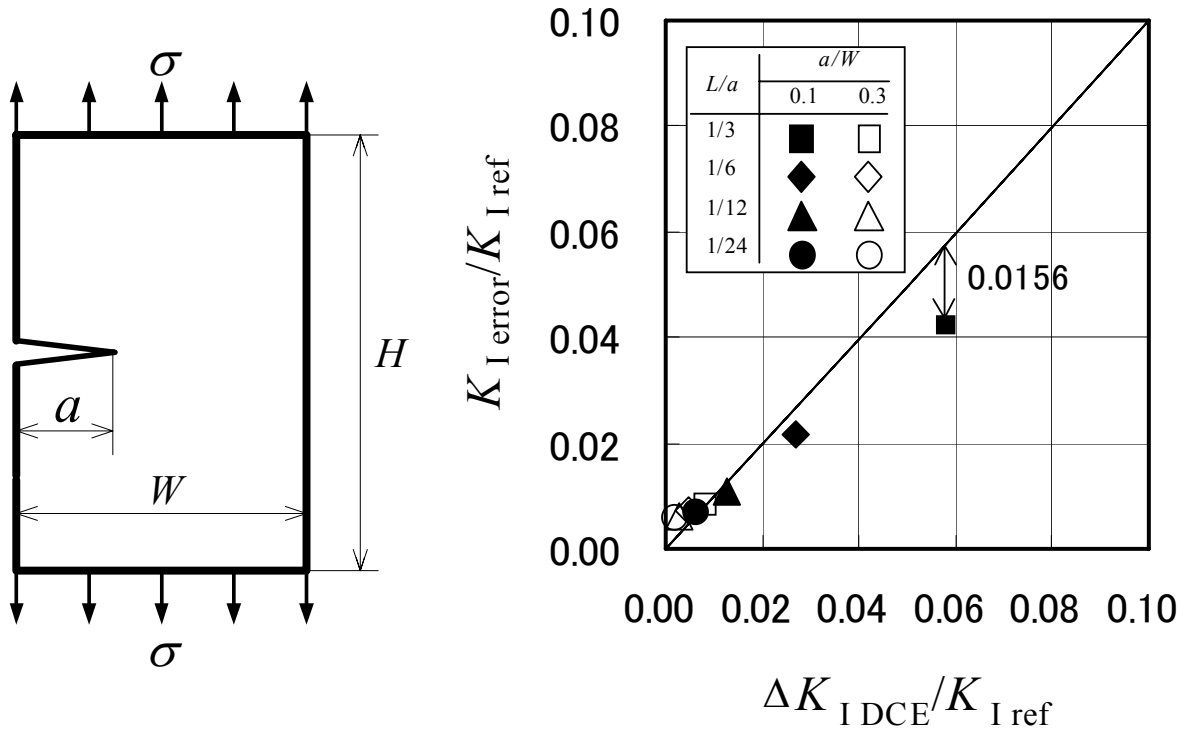

Fig. 2. Actual SIF error $K_{\mathrm{I\,error}}$ and DCE Index $\Delta K_{\mathrm{I\,DCE}}$ ($H/W = 2$, $m = 16$, $\nu = 0.3$).

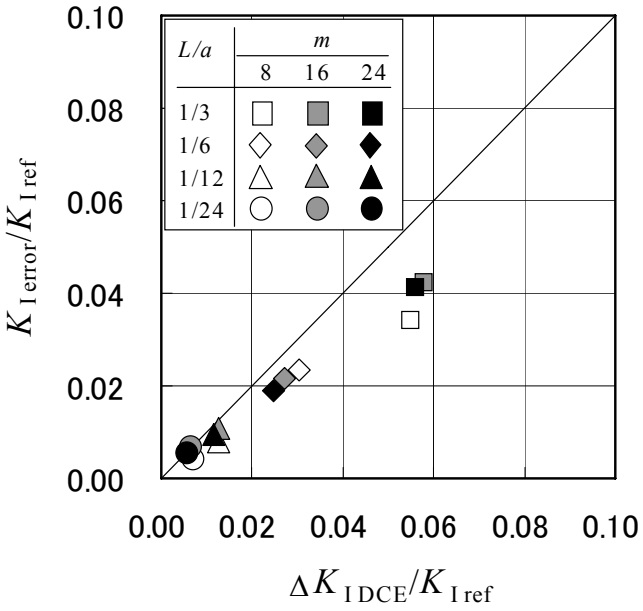

Fig. 3. Effect of singular element number m on actual SIF error $K_{\mathrm{I\,error}}$ and DCE Index $\Delta K_{\mathrm{I\,DCE}}$ (for $a/W = 0.1$ in Fig. 2)

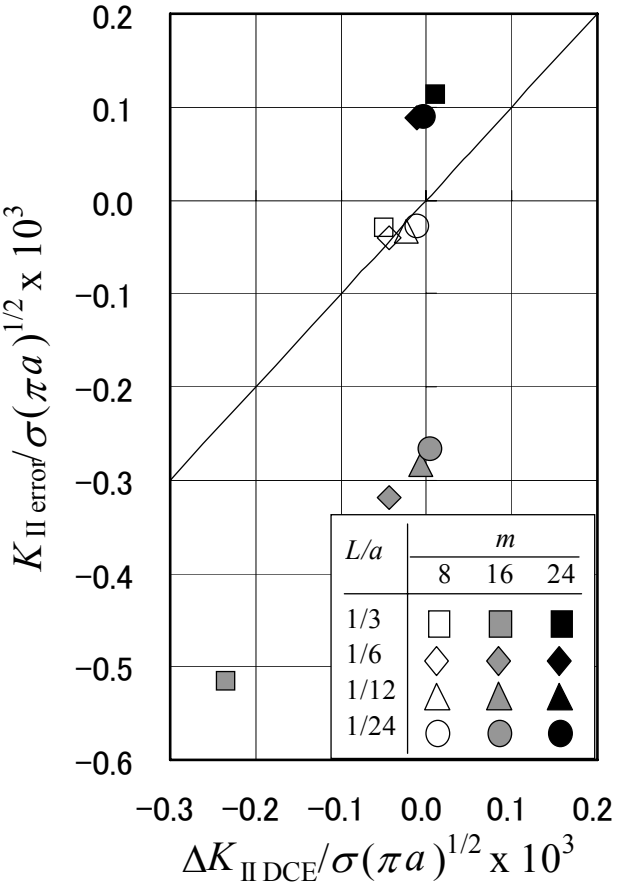

Fig. 4 Effect of singular element number m on actual SIF error $K_{\mathrm{II\,error}}$ and DCE Index $\Delta K_{\mathrm{II\,DCE}}$ (for $a/W = 0.1$ in Fig. 2)

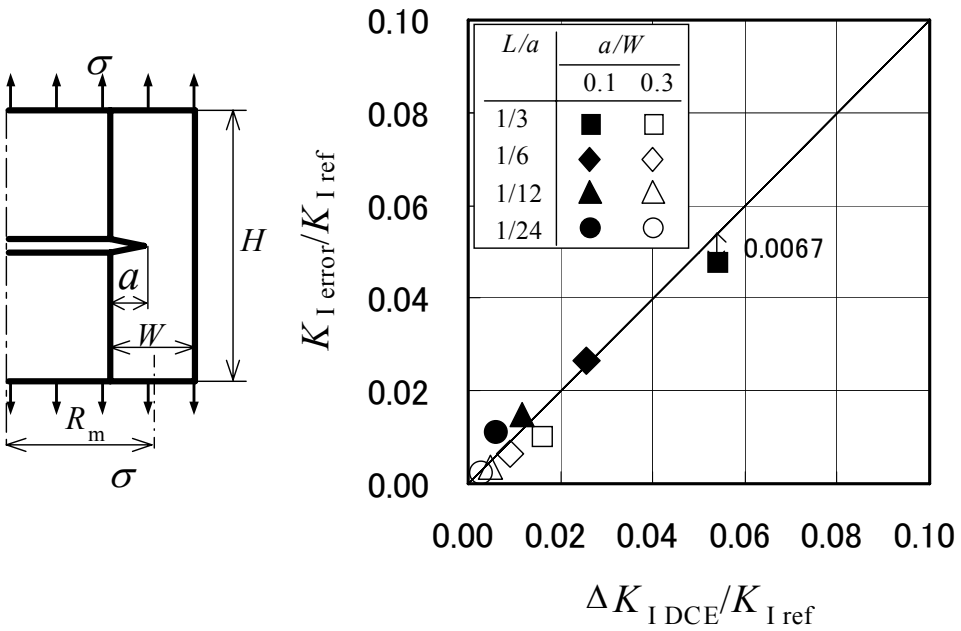

Fig. 5. Actual SIF error $K_{\text{I error}}$ and DCE Index $\Delta K_{\text{I DCE}}$ (R_m/W= 9.5, H/W = 16, m = 16, ν = 0.3).

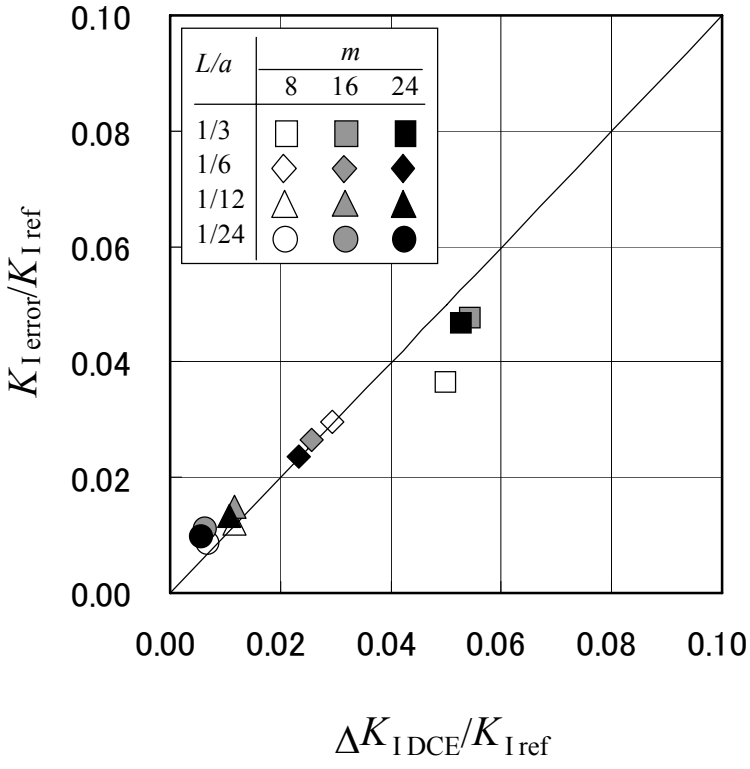

Fig. 6. Effect of singular element number m on actual SIF error $K_{\text{I error}}$ and DCE Index $\Delta K_{\text{I DCE}}$ (for a/W = 0.1 in Fig. 5).

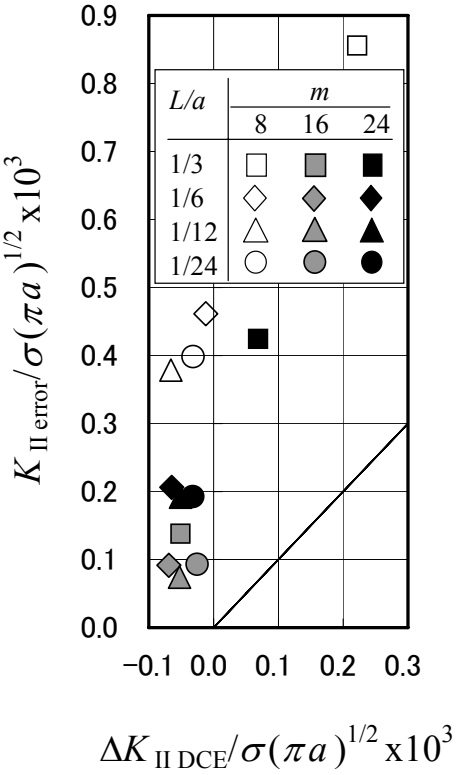

Fig. 7. Effect of singular element number m on actual SIF error $K_{\mathrm{II\,error}}$ and DCE Index $\Delta K_{\mathrm{II\,DCE}}$ (for $a/W = 0.1$ in Fig. 5)

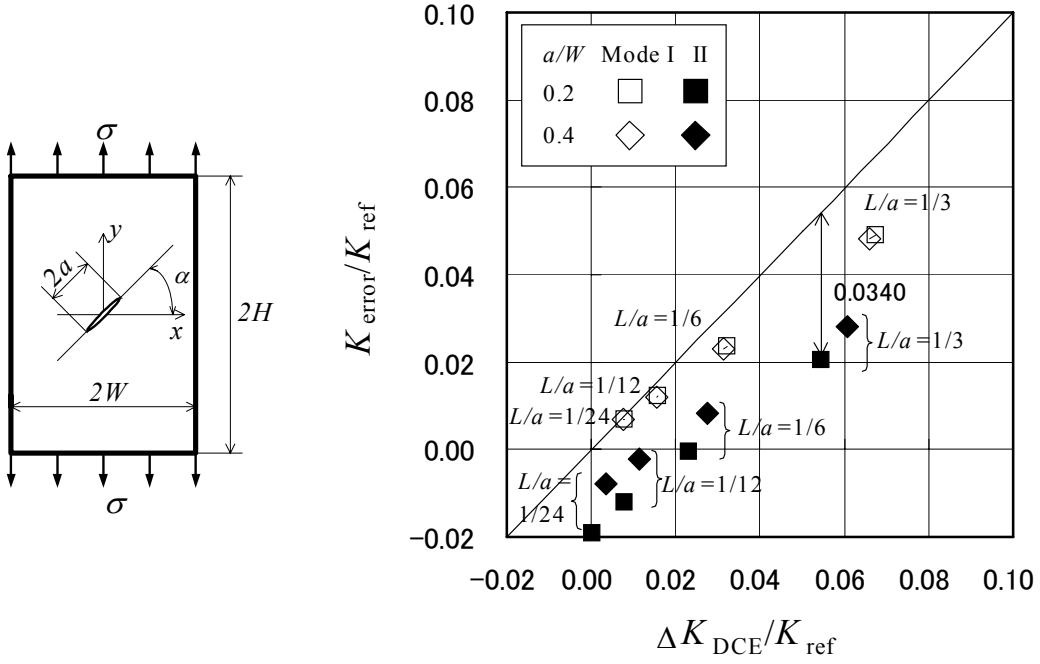

Fig. 8. Actual SIF error K_{error} and DCE Index ΔK_{DCE} ($H/W = 2$, m=24, α=30°, ν = 0.3).

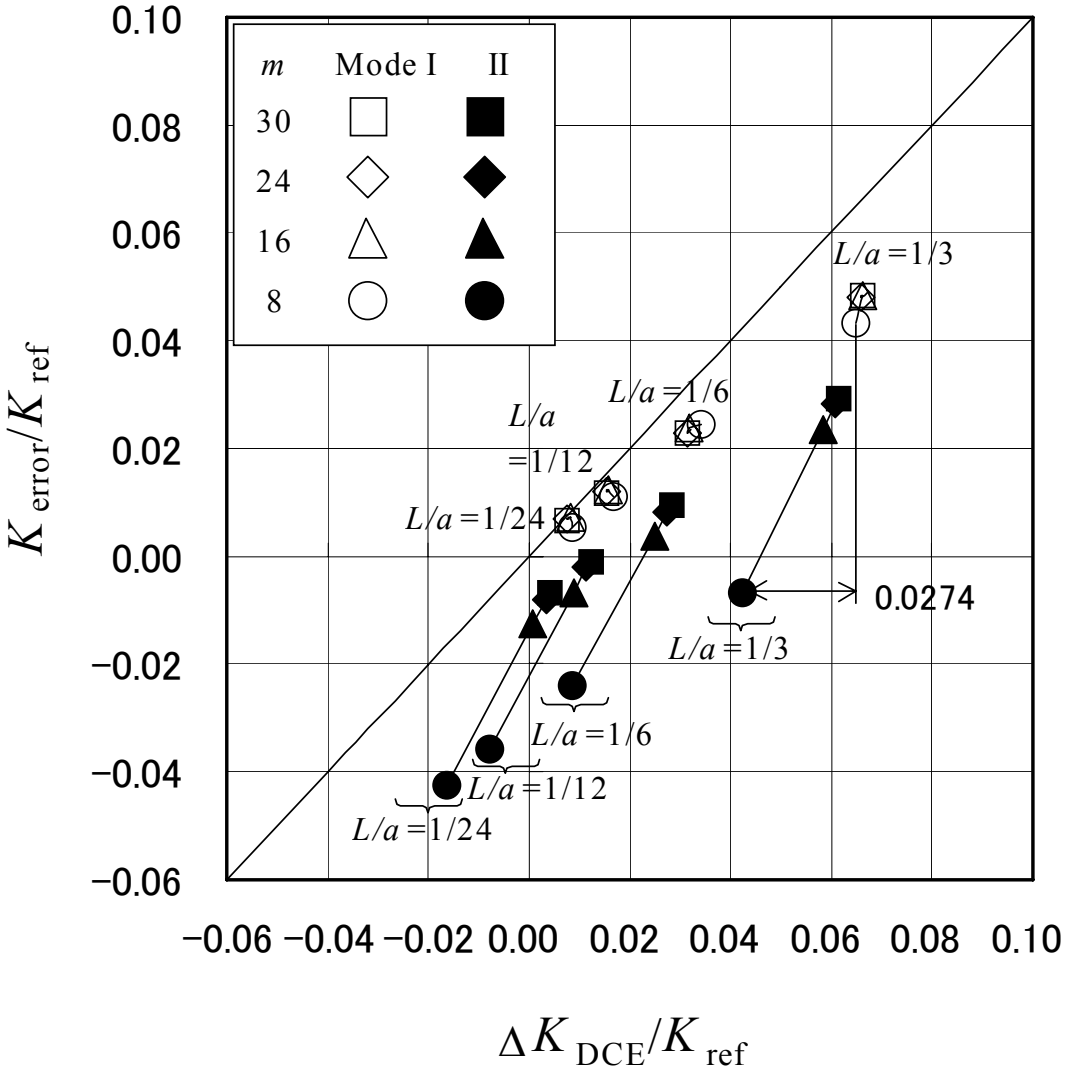

Fig. 9. Effect of singular element number m on actual SIF error K_{error} and DCE Index ΔK_{DCE} (for $a/W = 0.4$)

Table 1. Concrete values for Fig. 2 ($H/W = 2$, $m = 16$, $\nu = 0.3$)

a/W	$K_{I\mathrm{ref}}/\{\sigma(\pi a)^{1/2}\}$	L/a	$\Delta K_{I\mathrm{DCE}}/K_{I\mathrm{ref}}$	$K_{I\mathrm{error}}/K_{I\mathrm{ref}}$
0.1	1.196	1/3	0.0579	0.0423
		1/6	0.0271	0.0216
		1/12	0.0125	0.0108
		1/24	0.0065	0.0068
0.3	1.655	1/3	0.0083	0.0084
		1/6	0.0049	0.0072
		1/12	0.0027	0.0061
		1/24	0.0018	0.0058

Table 2. Concrete values for Fig. 3 ($a/W = 0.1$, $K_{Iref}/\sigma(\pi a)^{1/2} = 1.196$, $H/W = 2$, $\nu = 0.3$)

m	L/a	$\Delta K_{IDCE}/K_{Iref}$	K_{Ierror}/K_{Iref}
8	1/3	0.0548	0.0342
	1/6	0.0303	0.0234
	1/12	0.0126	0.0080
	1/24	0.0071	0.0043
16	1/3	0.0579	0.0423
	1/6	0.0271	0.0216
	1/12	0.0125	0.0108
	1/24	0.0065	0.0068
24	1/3	0.0559	0.0412
	1/6	0.0246	0.0189
	1/12	0.0115	0.0094
	1/24	0.0057	0.0056

Table 3. Concrete values for Fig. 4 ($a/W = 0.1$, $H/W = 2$, $\nu = 0.3$)

m	L/a	$\Delta K_{II\ DCE}/\sigma(\pi a)^{1/2}$ x 10^3	$K_{II\ error}/\sigma(\pi a)^{1/2}$ x 10^3
8	1/3	-0.0497	-0.0293
	1/6	-0.0443	-0.0401
	1/12	-0.0232	-0.0330
	1/24	-0.0116	-0.0271
16	1/3	-0.2359	-0.5152
	1/6	-0.0441	-0.3185
	1/12	-0.0065	-0.2829
	1/24	0.0047	-0.2660
24	1/3	0.0095	0.1144
	1/6	-0.0117	0.0878
	1/12	-0.0061	0.0898
	1/24	-0.0035	0.0903

Table 4. Concrete values for Fig. 5 (R_m/W= 9.5, H/W = 16, m = 16, ν = 0.3)

a/W	$K_{I\mathrm{ref}}/\{\sigma(\pi a)^{1/2}\}$	L/a	$\Delta K_{I\mathrm{DCE}}/K_{I\mathrm{ref}}$	$K_{I\mathrm{error}}/K_{I\mathrm{ref}}$
0.1	1.158	1/3	0.0543	0.0476
		1/6	0.0257	0.0266
		1/12	0.0117	0.0148
		1/24	0.0063	0.0111
0.3	1.392	1/3	0.0161	0.0101
		1/6	0.0091	0.0064
		1/12	0.0048	0.0034
		1/24	0.0029	0.0024

Table 5. Concrete values for Fig. 6 (a/W = 0.1, $K_{I\mathrm{ref}}/\sigma(\pi a)^{1/2}$ = 1.158, R_m/W= 9.5, H/W = 16, ν = 0.3)

m	L/a	$\Delta K_{I\mathrm{DCE}}/K_{I\mathrm{ref}}$	$K_{I\mathrm{error}}/K_{I\mathrm{ref}}$
8	1/3	0.0499	0.0366
	1/6	0.0294	0.0297
	1/12	0.0117	0.0120
	1/24	0.0069	0.0087
16	1/3	0.0543	0.0476
	1/6	0.0257	0.0266
	1/12	0.0117	0.0148
	1/24	0.0063	0.0111
24	1/3	0.0526	0.0467
	1/6	0.0233	0.0235
	1/12	0.0107	0.0133
	1/24	0.0056	0.0098

Table 6. Concrete values for Fig. 7 (a/W = 0.1, R_m/W= 9.5, H/W = 16, ν = 0.3)

m	L/a	$\Delta K_{II\,\mathrm{DCE}}/\sigma(\pi a)^{1/2}$ x 10^3	$K_{II\,\mathrm{error}}/\sigma(\pi a)^{1/2}$ x 10^3
8	1/3	0.2216	0.8556
	1/6	-0.0118	0.4615
	1/12	-0.0658	0.3784
	1/24	-0.0315	0.3983
16	1/3	-0.0509	0.1383
	1/6	-0.0688	0.0918
	1/12	-0.0523	0.0742
	1/24	-0.0253	0.0933
24	1/3	0.0689	0.4244
	1/6	-0.0647	0.2063
	1/12	-0.0508	0.1917
	1/24	-0.0318	0.1926

Table 7. Concrete values for Fig. 8 ($H/W = 2$, m=24, α=30°, $\nu = 0.3$).

a/W	$K_{\mathrm{I ref}}/\{\sigma(\pi a)^{1/2}\}$	$K_{\mathrm{II ref}}/\{\sigma(\pi a)^{1/2}\}$	L/a	$\Delta K_{\mathrm{I DCE}}/K_{\mathrm{I ref}}$	$K_{\mathrm{I error}}/K_{\mathrm{I ref}}$	$\Delta K_{\mathrm{II DCE}}/K_{\mathrm{II ref}}$	$K_{\mathrm{II error}}/K_{\mathrm{II ref}}$
0.2	0.7730	0.4367	1/3	0.0673	0.0491	0.0547	0.0206
			1/6	0.0322	0.0235	0.0231	-0.0004
			1/12	0.0158	0.0122	0.0079	-0.0120
			1/24	0.0079	0.0069	0.0003	-0.0192
0.4	0.8456	0.4497	1/3	0.0659	0.0482	0.0607	0.0282
			1/6	0.0313	0.0230	0.0274	0.0082
			1/12	0.0154	0.0119	0.0115	-0.0021
			1/24	0.0077	0.0068	0.0033	-0.0079

Table 8. Concrete values for Fig. 9 ($a/W = 0.4$, $H/W = 2$, α=30°, $\nu = 0.3$, $K_{\mathrm{I ref}}/\sigma(\pi a)^{1/2} = 0.8456$, $K_{\mathrm{II ref}}/\sigma(\pi a)^{1/2} = 0.4497$).

m	L/a	$\Delta K_{\mathrm{I DCE}}/K_{\mathrm{I ref}}$	$K_{\mathrm{I error}}/K_{\mathrm{I ref}}$	$\Delta K_{\mathrm{II DCE}}/K_{\mathrm{II ref}}$	$K_{\mathrm{II error}}/K_{\mathrm{II ref}}$
8	1/3	0.0648	0.0432	0.0423	-0.0067
	1/6	0.0342	0.0246	0.0086	-0.0239
	1/12	0.0167	0.0112	-0.0077	-0.0358
	1/24	0.0086	0.0053	-0.0164	-0.0425
16	1/3	0.0662	0.0485	0.0582	0.0236
	1/6	0.0318	0.0237	0.0249	0.0038
	1/12	0.0158	0.0125	0.0088	-0.0067
	1/24	0.0081	0.0074	0.0006	-0.0126
24	1/3	0.0659	0.0482	0.0607	0.0282
	1/6	0.0313	0.0230	0.0274	0.0082
	1/12	0.0154	0.0119	0.0115	-0.0021
	1/24	0.0077	0.0068	0.0033	-0.0079
30	1/3	0.0662	0.0484	0.0614	0.0294
	1/6	0.0313	0.0230	0.0284	0.0095
	1/12	0.0153	0.0118	0.0122	-0.0009
	1/24	0.0076	0.0067	0.0041	-0.0067